Optimization of purine-nitrile TbcatB inhibitors for use in vivo and evaluation of efficacy in murine models

Jeremy P. Mallari [a,b], Fangyi Zhu [b], Andrew Lemoff [b], Marcel Kaiser [c], Min Lu [b], Reto Brun [c], R. Kiplin Guy [a,b,*]

[a] Graduate Program in Chemistry and Chemical Biology, University of California, San Francisco CA 94143-2280, United States
[b] Department of Chemical Biology and Therapeutics, St. Jude Children's Research Hospital, Memphis TN, 38105, United States
[c] Swiss Tropical and Public Health Institute, Socinstrasse 57, 4002 Basel, Switzerland

ARTICLE INFO

ABSTRACT

There are currently only four clinical drugs available for treating human African trypanosomiasis (HAT), three of which were developed over 60 years ago. Despite years of effort, there has been relatively little progress towards identifying orally available chemotypes active against the parasite in vivo. Here, we report the lead optimization of a purine-nitrile scaffold that inhibits the essential TbcatB protease and its evaluation in murine models. A lead inhibitor that had potent activity against the trypanosomal protease TbcatB in vitro and cultured parasites ex vivo was optimized by rationally driven medicinal chemistry to an inhibitor that is orally available, penetrates the CNS, has a promising pharmacokinetic profile, and is non-toxic at 200 mg/kg in a repeat dosage study. Efficacy models using oral administration of this lead inhibitor showed a significantly increased survival time in *Trypanosoma brucei brucei* infected mice but little effect on *Trypanosoma brucei rhodesiense* infected mice.

© 2010 Elsevier Ltd. All rights reserved.

1. Introduction

The four drugs (melarsoprol, eflornithine, pentamidine, and suramin) currently approved for treating human African trypanosomiasis (HAT)[†] have toxic side effects and require intravenous administration, which is difficult in the rural areas where HAT is endemic.[1] In addition, only melarsoprol is effective against the CNS stage of both forms of HAT.[1,2] These limitations drive the need to discover and develop new chemotypes to treat sleeping sickness, especially those with lower toxicity, improved oral absorption, and CNS penetration. Much of the current effort for HAT inhibitor development has focused on reoptimization of established chemical scaffolds, especially the dicationic aryl bis-amidines. In fact, other than eflornithine the only new small molecules to move into clinical trials for HAT since the 1970's are fexinidazole and the pentamidine prodrug DB289 (pafuramidine).[3–7] There have been few novel inhibitor scaffolds that show in vivo efficacy against a murine *Trypanosoma brucei* infection, and even fewer scaffolds with established oral efficacy. Some examples of chemotypes active in animal models include buthionine sulfoximine,[8] which targets gamma glutamyl cysteine synthetase; ascofuranone,[9,10] which targets ubiquinol oxidase; benzyl diamino pyrimidines,[11] which target dihydrofolate reductase; 6-diazo-5-oxo-L-norleucine and α-amino-3-chloro-4,5-dihydro-5-isoxazoleacetic acid,[12] which target cytidine triphosphate synthetase; diazomethane peptide analogues,[13,14] which target multiple cysteine proteases; D-carnitine,[15] which inhibits glycolysis; and S-adenosyl-L-methionine analogues,[16] which target polyamine metabolism. Among these leads, only DB289, D-carnitine, and ascofuranone, have demonstrated efficacy by an oral route. Only DB289 and ascofuranone are curative, and both require multiple daily treatments to clear an infection.[5–7,10] Despite the early success of these compounds, only DB289 is particularly amenable to medicinal chemistry and further development. In addition, DB289 has poor CNS permeability and is therefore not effective against late stage infections. There is clearly a pressing need for the identification of novel orally available and CNS permeable trypanocides.

We have previously reported a purine-nitrile scaffold with potent activity against cultured trypanosomes.[17,18] These compounds were targeted to the trypanosomal protease TbcatB, one of two papain-like cysteine proteases in the parasite. TbcatB is essential for parasite growth and facilitates iron acquisition via lysozomal degradation of host transferrin.[19,20] Prior work in our group optimized potency and selectivity against TbcatB and demonstrated a strong correlation between TbcatB inhibition and trypanocidal activity. This series of inhibitors also kills cultured parasites with a high degree of selectivity relative to multiple mammalian cell lines.[17,18]

Herein, we report the optimization of the absorption, distribution, metabolism, and excretion (ADME) of this inhibitor series using both in vitro methods and an in vivo murine model. A total of six inhibitors were evaluated for acute toxicity in Balb/C mice and found to have no adverse event threshold levels (NAETL) of greater than 200 mg/kg. ADME of a test set of three compounds was examined and these data indicated that oxidation at the N9 side chain was a major issue for this inhibitor series. Modifications to the N9 side chain were tested for in vivo and in vitro stability, leading to the development of a best candidate **3f**. Inhibitor **3f** was optimized for oral absorption and metabolic stability while maintaining potent trypanocidal activity ($EC_{50} = 0.53$ μM). Single oral doses of **3f** at 1000 mg/kg are non-toxic. Concentrations of exceeding 10 μM could be achieved in both the plasma and brain tissue, and these levels persisted for over 24 h following a single 200 mg/kg oral dose of the lead inhibitor. This compound was also characterized in a repeat dosage study, and no negative symptoms were observed after daily treatments of 200 mg/kg for 10 consecutive days. Finally, **3f** was evaluated for efficacy in *Trypanosoma brucei brucei* infected mice and, although the treatment was not curative, post-infection survival time was significantly increased. However, the compound was not active in vivo against a *Trypanosoma brucei rhodesiense* infection.

2. Materials and methods

2.1. Chemistry

Purine-nitriles were synthesized using the general routes previously described (Scheme 1).[17,18] Briefly, **1** was reacted with the appropriate amine in 2-butanol to install the 6-amino substituent. The crude reaction mixture was concentrated in vacuo and resuspended in DMF with K_2CO_3. Heating this mixture with the desired alkyl bromide afforded alkylation at N9. Purification was accomplished by silica medium pressure chromatography giving overall yields for the two reactions ranging from 25% to 60%. Subsequent reaction with sodium cyanide in DMSO with microwave acceleration afforded nitriles **3a–f**, which were purified by preparative C_{18} chromatography with yield of 30–70%. Suzuki coupling of **3a** and 2,6-dimethylphenylboronic acid was performed with Na_2CO_3 and $Pd(PPh_3)_4$ in 1,4-dioxane with microwave acceleration to give inhibitor **4a**. The target inhibitor **4a** was purified by preparative C_{18}

chromatography with a resulting yield of 60%. Purity of all compounds was confirmed by two orthogonal analytical LC/MS procedures, using both C_4 and C_{18} columns.

2.2. In vitro inhibitor testing

Compounds were selected for testing in a mouse model of toxicity based on protease inhibition profile, trypanocidal potency, cellular therapeutic index, and stability profile, as previously described.[17,18] Prior to testing in mice, each inhibitor was evaluated using an in vitro ADME assay panel to identify potential in vivo liabilities. Aqueous solubility and passive permeability (PAMPA) were determined using a physiologically relevant pH range to predict oral absorption and cell membrane permeability. Compound stability was tested in DMSO, PBS, and mouse plasma to assess non-metabolic degradation. In addition, stability in liver microsomes, hemolytic activity, and cytotoxicity was determined according to previously reported methods to predict expected hepatic CL and potential toxicity.[18,21–25]

2.3. Formulation

Inhibitor formulations were developed using a standardized high throughput UPLC based assay with either UV or MS detection.[22] Briefly, several combinations of three different organic co-solvents (ethanol, propylene glycol, and PEG 400) were diluted in various buffered aqueous solutions (pH 4, 7.4, and 9) and dispensed into a 96-well plate (Supplementary data). These co-solvents effectively solubilize hydrophobic compounds and are compatible with IV, IP, and oral routes of administration. A DMSO inhibitor stock solution of each compound was then added to each well to a final concentration of 1% DMSO and 10 mM inhibitor. The plate was sealed and agitated on an orbital shaker overnight then centrifuged to pellet undissolved compound. A sample was then taken from the center depth of each well for UPLC analysis to determine the concentration of inhibitor in solution.

2.4. Preliminary in vivo ADME characterization

Initial in vivo studies were designed to quickly provide a preliminary assessment of acute toxicity, inhibitor metabolites, and semi-quantitative oral absorption and plasma exposure. Studies
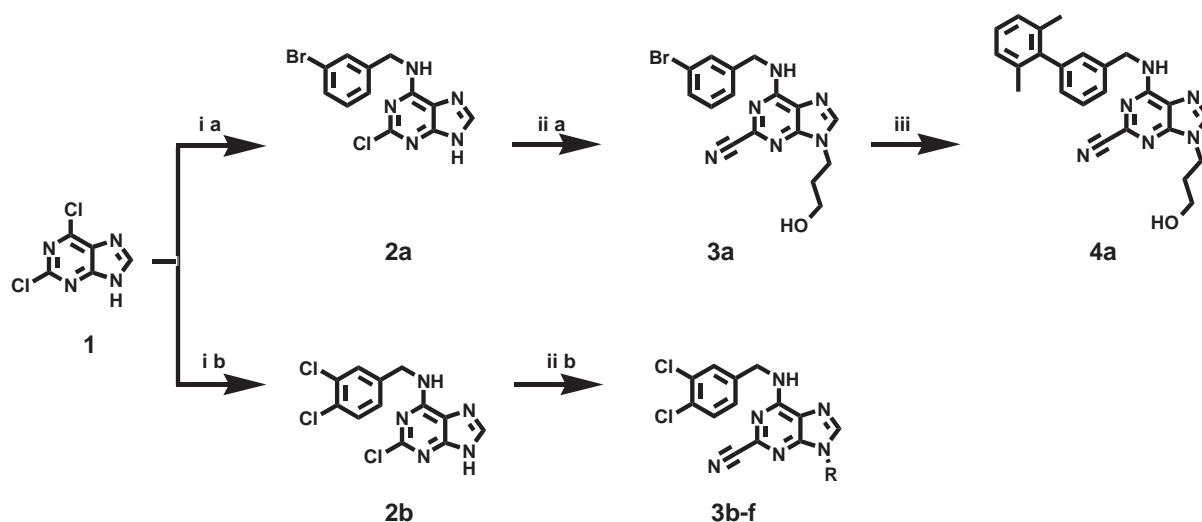
Scheme 1. Synthesis of purine-nitriles. Reagents and conditions: (i) (a/b) 3-bromobenzylamine or 3,4-dichlorobenzylamine, 2-butanol, 60 °C, 3–12 h; (ii) (a/b) alkyl bromide or 3-hydroxypropylbromide, K_2CO_3, DMF, 60 °C, 10–16 h; then NaCN, DMSO, μW, 180 °C, 160 W, 5–20 min; (iii) 2,6-dimethylphenylboronic acid, Na_2CO_3, $Pd(PPh_3)_4$, 1,4-dioxane, μW, 150 °C, 300 W, 5–40 min.

were performed using 12 mice per compound, which were treated in a four-stage dose escalation study. One advantage of the experimental design is that acute toxicity data are collected simultaneously with preliminary pharmacokinetic data, using the same animals.

The maximum tolerated dosage (MTD) for oral administration of each inhibitor was determined by testing increasing dosages starting with vehicle only, followed by 50, 100, and 200 mg/kg. Following treatment, mice were observed using a modified Irwin Functional Observational Battery (FOB) for 15 min for acute adverse symptoms before continuing the dose escalation.[26] All mice were monitored for 48 h after completion of the dose escalation. For each dosage group, a single retro orbital bleed of approximately 0.1 ml was collected for UPLC–MS analysis from one mouse at 1, 2, and 4 h after drugging. At 48 h animals were sacrificed, a terminal blood draw was collected by cardiac puncture, and a gross necropsy was performed. The blood sample was used for complete blood count (CBC) and serum chemistry analysis, as well as to provide a final PK time point.

2.5. Efficacy studies

In vivo efficacy against *T.b. brucei* was modeled using an established system.[13,27] On day 0, 16 female Balb/C mice, aged 10–12 weeks, were infected with *T.b. brucei* (strain 221) by intraperitoneal injection of approximately 800 parasites. Infected mice were randomly selected for treatment with either **3f** (200 mg/kg) or vehicle on days 0–4. Blood was collected by saphenous vein puncture every third day, starting on day 4, to measure parasitemia by hemocytometer. Animals displaying symptoms indicative of unacceptably high parasitemia were euthanized. In vivo efficacy against *T.b. rhodesiense* (strain STIB900) was modeled in female NMRI mice. Mice were infected by ip injection of 2×10^4 parasites on day 0

and treated on days 3, 4, 5, and 6 with **3f** (50, 100, or 200 mg/kg) or vehicle only. Four mice were used for each dosage group, and survival time was determined as described above (Fig. 2).

3. Experimental

3.1. 6-((3,4-Dichlorobenzyl)amino)-9-(4,4,4-trifluorobutyl)-9H-purine-2-carbonitrile (3f)

3-(Trifluoromethyl)propyl bromide was purchased from Matrix Scientific. All other chemicals were purchased from Sigma–Aldrich. All reaction solvents were anhydrous. LC/MS data were collected on a Waters system using XTerra C_{18} columns (MeOH/H_2O, 1% HCOOH). Synthesis was performed as previously described.[17,18] Briefly, 2,6 dichloropurine **1** (0.25 g, 1.3 mmol) was suspended in of 2-butanol (3.9 ml, 0.34 M) and treated with the appropriate benzylamine by drop-wise addition (3.9 mmol, 3.0 equiv). The reactions were stirred for 3–12 h at 60 °C with monitoring by thin layer chromatography (silica gel 60). The crude product mixture was concentrated under vacuum and resuspended in anhydrous DMF (5 ml, 0.26 M). K_2CO_3 (solid, 0.54 g, 3.9 mmol, 3.0 equiv) was added, followed by drop-wise addition of the desired alkyl bromide (5.2 mmol, 4.0 equiv). The reaction was stirred 12–18 h at 60 °C and monitored by LC/MS. The crude reaction was concentrated under vacuum and purified by flash chromatography (30:1 DCM/MeOH v/v) using 40 M columns (Biotage) on a Biotage SP1 flash chromatography instrument to give a waxy solid (60% yield).

The purified intermediate (2-chloro-*N*-(3,4-dichlorobenzyl)-9-(4,4,4-trifluorobutyl)-9H-purin-6-amine) 2-chloro-*N*-(3,4-dichlorobenzyl)-9-(4,4,4-trifluorobutyl)-9H-purin-6-amine (0.5 mmol) was dissolved in DMSO (5.0 ml, 0.1 M) in a 5 ml microwave reaction vial (Biotage). Sodium cyanide (170 mg, 3.5 mmol, 7.0 equiv) was added. The vial was sealed and heated to 180 °C for increments
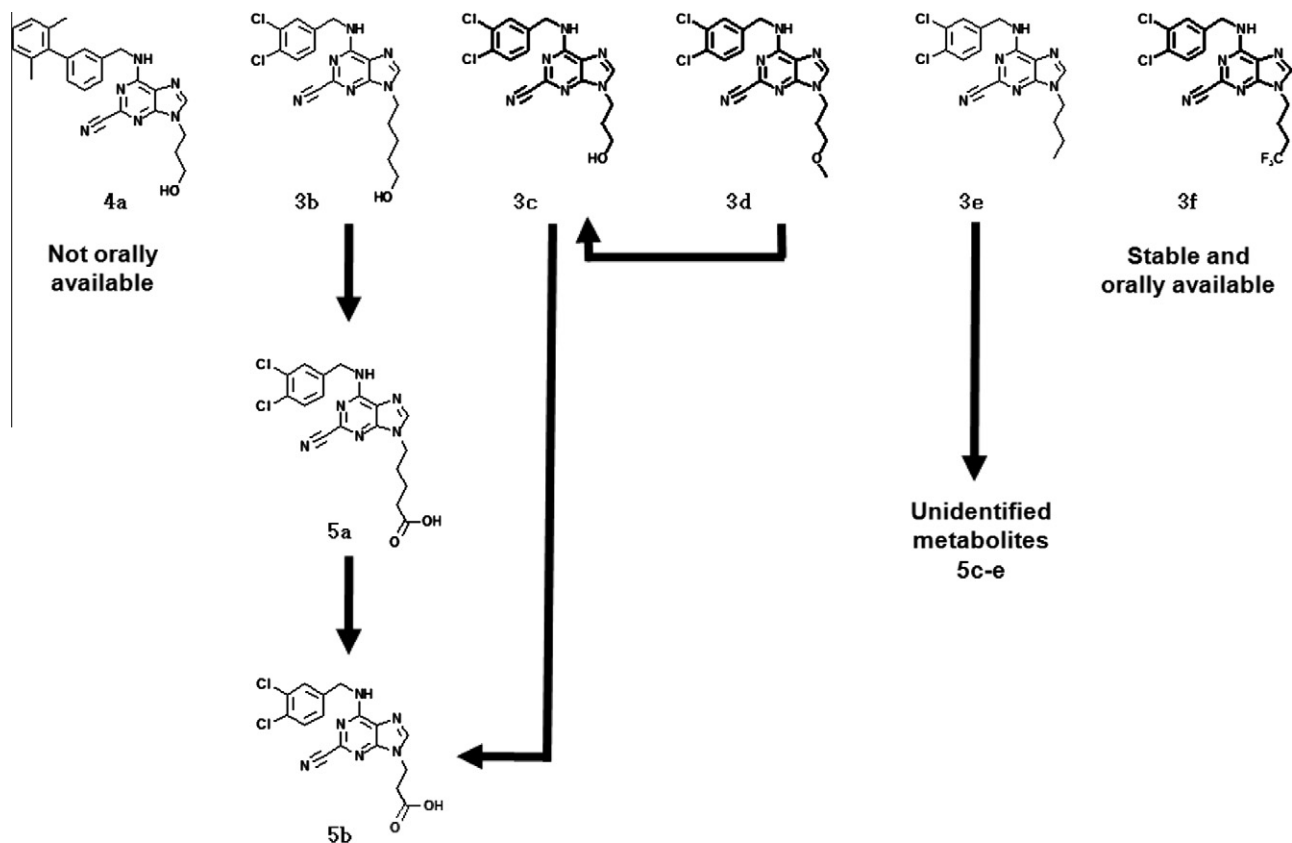

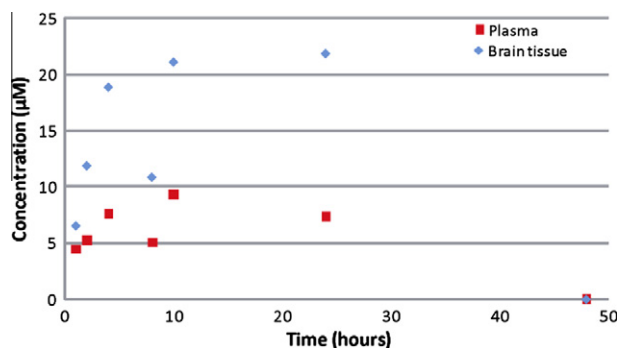**Figure 1.** In vivo inhibitor metabolism.

Figure 2. Brain and plasma concentration of inhibitor **3f** dosed at 200 mg/kg.

of 10 min in a Biotage Initiator microwave until the reaction was complete as shown by LC/MS, a total of 30–90 min. The crude product mixture was decanted from insoluble NaCN and purified by reverse-phase HPLC (Waters XTerra preparative C_{18} column, ACN/H_2O, 1% HCOOH, linear gradient from 40–70% ACN) to afford nitrile **3f** with a yield of 70%.

3.2. ¹H NMR peak listing for inhibitor 3f

¹H NMR ($(CD_3)_2SO$) (400 MHz): δ 9.02 (1H, m), 8.46 (1H, s), 7.60 (2H, m), 7.34 (1H, d, J = 8.0 Hz), 4.67 (2H, d, J = 6.0 Hz), 4.27 (2H, t, J = 6.8 Hz), 2.34 (2H, m), 2.06 (2H, quintet, J = 7.6 Hz) LC/MS: M+H⁺: 429.15.

3.3. Cloning and expression of TbcatB

TbcatB was cloned, expressed, and purified as previously described.[18]

3.4. Enzyme inhibition assays

Inhibitors were screened against TbcatB, rhodesain, human cathepsin B, and human cathepsin L as previously described.[18,20]

3.5. Cell proliferation assays

Inhibitors were screened against *T.b. brucei*, HEK 293, Hep G2, BJ, and Raji as previously described.[18,20]

3.6. Liver microsomal stability

Microsomal stability was determined as previously described[21,23] with some modification. 0.63 ml of liver microsome protein (20 mg/ml, female CD-1 mice, BD Biosciences) was mixed with 0.05 ml of 0.5 M EDTA solution and 19.32 ml potassium phosphate buffer (0.1 M, pH 7.4, 37 °C) to make 20.00 ml of liver microsome solution. One part of 10 mM DMSO compound stock was mixed with 4 part of acetonitrile to make 2 mM diluted compound stock in DMSO and acetonitrile. 30.4 µl diluted compound stock was added to 2.4 ml liver microsomal solution and vortexed to make microsomal solution with compound. 180 µl of the microsomal solutions with different compounds were dispensed into respective rows of a 96-well storage plate (pION Inc., MA). For 0 h time point, 450 µl pre-cooled acetonitrile (−20 °C) with internal standard (100 µM caffeine) was added to the first three columns before the reaction starts. 1.25 ml of microsome assay solution A (BD Biosciences) was combined with 0.25 ml of solution B (BD Biosciences) in 3.5 ml of potassium phosphate buffer (0.1 M, pH 7.4). 45 µl of this solution was added to each well of the 96-well storage plate (reaction plate). Liquid in the first three columns was moved to another storage plate (quenched plate). The

reaction plate was incubated at 37 °C and shaken at a speed of 60 rpm. 0.5 h, 1 h, 2 h time points were taken. At each time point, 450 µl pre-cooled acetonitrile was added to three rows in the reaction plate, and the liquid was then transferred to the quenched plate. The quenched plate was then centrifuged (model 5810R, Eppendorf, Westbury, NY) at 4000 rpm for 20 min. 200 µl supernatant was transferred to a 96-well plate and analyzed by UPLC–MS (Waters Inc., Milford, MA). The compounds and internal standard were detected by SIR. The log peak area ratio (compound peak area/internal standard peak area) was plotted against time and the slope was determined to calculate the elimination rate constant [$k = (−2.303)$ *slope]. The half life (h) was calculated as $t_{1/2}$ = 0.693/k.

3.7. Determination of hemolytic potential

Inhibitors were tested as previously reported.[23] Briefly, 1 ml of whole human blood was centrifuged at 1000g for 5 min. The supernatant was decanted and the pellet was washed three times with 1 ml PBS, pH 7.4. 400 µl human erythrocytes were resuspended in 9.6 ml PBS. In a 96-well plate, 2 µl of 1 mM analyte was added to 98 µl PBS and mixed. In the first 2 rows of the 96-well plate, 100 µl PBS was added as a negative control. 100 µl of resuspended human erythrocytes were added to each well. Final assay hematocrit was 2% and analyte concentration was 10 µM. 0.4% saponin was used as a positive control for full hemolysis and 1%, 10% and 20% ethanol utilized as partial hemolysis controls. The plate was incubated at 37 °C with shaking at 60 rpm for 5 h and then centrifuged at 1000g for 5 min. 75 µl supernatant from each well was transferred to a 96-well UV plate (Corning). 75 µl supernatant from saponin well was added to wells A1 and B1, and serial diluted along the row to wells A11 and B11. Absorbance at 414 nm was determined for each well, and percent hemolysis was determined using a standard calibration curve. All data was collected in triplicate.

3.8. Metabolite identification

All metabolite identification was performed using a Waters Acquity UPLC system (Waters, Milford, MA) coupled to either a Waters Acquity single quadrupole mass spectrometer or a Waters Acquity triple quadrupole mass spectrometer, both fitted with an electrospray ionization (ESI) source. Chromatographic separations were achieved on a 21 × 50 mm, 1.7 µm Waters Acquity BEH column. The column eluent was split after the column, with half going to the mass spectrometer and half going to a PDA detector. All analyses were performed in positive ion mode. Instrument control, data acquisition, and data processing were performed using Masslynx v. 4.1.

Mobile phase for the single quadrupole MS was 0.1% formic acid in water and methanol. The proportion of methanol was increased from 40% to 100% over 4 min. Mass spectra were acquired over a range of m/z = 110–600. The triple quadrupole MS mobile phase consisted of 0.1% formic acid in water and 0.1% formic acid in acetonitrile. The proportion of acidified acetonitrile was increased from 10% to 90% over 1.8 min, and brought back to 10% over 0.2 min. MS/MS spectra were acquired over a range of m/z = 50–450. Collision energies were varied from 15–30 eV to achieve varying amounts of fragmentation to aid in structural elucidation.

3.9. Mouse MTD and chronic toxicity studies

Female balb/c mice aged 10–12 weeks were purchased from Charles River Laboratories and housed individually. Food and water were provided ad libitum. Inhibitors **3b** and **3d** were suspended in 5% ethanol, 50% propylene glycol, and 45% PBS (pH

7.4). Compounds **3c** and **3e** were suspended in 10% ethanol, 10% propylene glycol, 40% PEG 400, and 40% PBS (pH 7.4). Compound **4a** was suspended in 10% ethanol, 10% propylene glycol, 40% PEG 400, and 40% sodium citrate (1 mM, pH 6.0). Compound **3f** was suspended in 20% ethanol, 40% propylene glycol, 10% PEG 400, and 30% PBS (pH 7.4). Oral dosing at 50, 100, 200, 400, and 1000 mg/kg was carried out with inhibitor suspensions of 10, 20, 40, 80, and 200 mg/ml, respectively. For each mouse, 0.1 ml of inhibitor suspension was given by oral gavage for every 20 g of animal weight. To determine the IV MTD for inhibitor **3f**, solubilized inhibitor was given by lateral tail vein injection (0.1 ml solution per 20 g animal). Dosing of **3f** at 2, 4 and 8 mg/kg was carried out with inhibitor solutions of 0.4, 0.8, and 1.6 mg/ml, respectively.

0.1 ml blood was collected retro-orbitally from a different mouse within each treatment group at 1, 2, and 4 h after treatment. Only one collection was made per mouse during the entire study period. In some cases the sample size was expanded to six animals and additional samples were collected at 8, 12, and 24 h. All samples were treated with EDTA. Mice were observed at 1, 2, 4, 8, 24, 32, and 48 h according to a modified FOB. Gait, alertness, respiration, piloerection, vasodilation, and vocalization were monitored and recorded at each time point. At 48 h the animals were sacrificed and a terminal cardiac bleed was collected from each animal. Plasma samples were prepared as previously described.[25] Briefly, each blood sample was centrifuged for 2 min at 10,000 rpm in a desktop centrifuge, and the plasma was collected. Plasma was diluted in three parts of ice cold acetonitrile, vortexed vigorously, and centrifuged at 13,000 rpm for 10 min in a desktop centrifuge. The supernatant was collected and inhibitor concentration was determined in a UV/HPLC based assay.

The chronic toxicity of **3f** was determined in a group of five mice treated by oral gavage with 200 mg/kg daily for 10 days. Surviving mice were monitored out until 30 days. One mouse from the cohort was euthanized and submitted for blood analysis and necropsy on day 10 and day 30, respectively.

3.10. Efficacy studies

Parasites were grown to a density of 10^7 parasites/ml in HMI-9 media supplemented with 10% fetal bovine serum (Omega), 10% Serum Plus (JRH Biosciences), and penicillin/streptomycin. Parasites were pelleted by centrifugation then resuspended and serially diluted in unsupplemented HMI-9 media to a density of 8×10^3 parasites/ml. Mice were inoculated by IP injection of 0.1 ml of this culture at 0 h on day 0. Mice weights were recorded and each animal was randomly assigned to either a drug treatment or vehicle only control group Mice were drugged by oral gavage with a suspension of inhibitor **3f** (40 mg/kg, final dose of 200 mg/kg) or with vehicle only (20% ethanol, 40% propylene glycol, 10% PEG 400, and 30% PBS (pH 7.4)). Gavage volume was 0.1 ml per 20 g animal weight. Oral dosing was continued once a day at 24, 48, 72, and 96 h post-infection. Blood was collected every third day starting on day 4 to monitor parasitemia. Approximately 10 µl of blood was collected by saphenous vein puncture in a heparinized collection tube. Blood samples were diluted 100 fold in PBS and parasite density was counted by hemocytometer. Animals displaying symptoms indicative of heavy parasitemia (extensive piloerection, lack of responsiveness) were euthanized by CO_2 asphyxiation followed cervical dislocation.

4. Results

An initial set of three inhibitors (**3b**, **3c**, and **4a**) was chosen for ADME characterization based on previously determined trypanocidal activity, in vitro therapeutic index, and TbcatB selectivity.[17,18]

Compounds were tested for hemolytic activity as well as stability in DMSO, PBS, mouse plasma, and liver microsomes. Solubility and PAMPA permeability were determined, and dosing formulations were developed for in vivo studies. In vivo studies assessed each inhibitor's metabolic stability, oral availability, plasma exposure, and MTD. Subsequent optimization was driven by these in vivo parameters. A total of six inhibitors (**3b–3f**, and **4a**) were tested in this study.
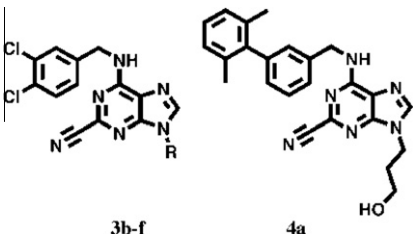
4.1. In vivo ADME optimization

ADME testing began with inhibitors **3b–c** and **4a**. Each of these compounds was non-toxic in cell proliferation and hemolysis assays, and stable in DMSO and PBS (pH 3, 5, and 7.4) over the course of the study (14 days). Stability of **3b**, **3c**, and **4a** in both microsomes and mouse plasma was modest (microsome $t_{1/2}$ = 0.53–1.08 h, plasma $t_{1/2}$ = 5.1–38.3 h) (Table 1). PAMPA flux values for **3b** and **3c** were reasonable, though it was not possible to determine a value for **4a** due to its low aqueous solubility (Table 2).

In vivo, the initial inhibitor set displayed no detectable plasma exposure due to either poor oral availability or poor metabolic stability. Blood samples of mice treated with **4a** did not show detectable amounts of either the inhibitor or potential inhibitor metabolites, suggesting little or no oral absorption. Inhibitors **3b** and **3c** were also not detected in the blood, although high levels (>50 µM) of a single, predominant, oxidatively modified metabolite (**5a** and **5b**, respectively) was observed for each compound (Supplementary data). MS/MS analysis indicated these metabolites arose from oxidation of the inhibitor's terminal hydroxyl groups on the N9 side chain to carboxylic acids **5a** and **5b** (Fig. 1). After oral dosing of **3c**, the parent inhibitor was completely converted to **5b** by the 1-h time point and no other metabolites were detectable. Following the oral dosing of **3b**, **5a** concentration peaked at 1 h, followed by a drop in **5a** levels and a corresponding increase in **5b** concentration at 2 and 4 h. **3b** also gives rise to a minor metabolite (m/z = 435), which appears to be the result of the hydroxylation of the N9 sidechain of **5a**. Low levels of an unidentified metabolite (m/z = 386) were also detected for **3c**. These data suggest that **3b** is first oxidized to **5a** then subsequently converted to **5b**, presumably by β-oxidation. The **5b** metabolite does not appear to give rise to any other species. These metabolic modifications are undesirable, as previous work has shown that such carboxylic acid derivatives are active against TbcatB (**5b** IC_{50} = 2.6 ± 0.6 µM) but inactive against the parasite (**5b** EC_{50} >25 µM), presumably due to poor cell permeability.

Taken together, these results indicate that those compounds that provided the best balance of in vitro characteristics have significant ADME liabilities that hinder their further development. The large and hydrophobic 6-amino biphenyl moiety of **4a**, the most TbcatB selective inhibitor in the series, is apparently responsible for the inhibitor's poor oral absorption. Likewise, the N9 hydroxyalkyl sidechains of inhibitors **3b–c**, which provide reasonable solubility and potency, are rapidly oxidized. Despite the instability of the **3b–c**, these compounds appear to have good oral absorption. Modification of the side chain alcohol was considered a more tractable strategy for mitigating these liabilities than attempting to address the poor oral absorption of the more hydrophobic subseries. Further efforts focused on optimizing the stability of the N9 side chain while leaving fixed the 3,4-dichlorobenzyl group at the 6-amino position.

Preventing side chain oxidation by replacing the hydroxyl of **3c** with the corresponding methyl ether **3d** was initially assessed. In vitro, this modification did not significantly improve microsomal stability ($t_{1/2}$ = 0.53 h) or PAMPA permeability, but did significantly improve plasma stability ($t_{1/2}$ = 40.9 h) relative to **3c** (Tables 1 and 2). In vivo, the parent compound **3d** was not detected after oral

Table 1
Inhibitor activity and stability in vitro

3b-f   4a

Inhibitor	R	EC$_{50}$ versus *T. brucei* (µM)	Therapeutic index (fold)	% Hemolysis	Plasma $t_{1/2}$ (h)	Microsome $t_{1/2}$ (h)
3b	5-Hydroxypentyl	0.38 ± 0.04	>20	0.70 ± 0.03	38.3	1.08 ± 0.09
3c	3-Hydroxypropyl	1.4 ± 0.1	>20	0.70 ± 0.05	5.1	0.60 ± 0.02
3d	3-Methoxypropyl	2.4 ± 0.4	>10	0.70 ± 0.08	40.9	0.53 ± 0.04
3e	*n*-Butyl	0.5 ± 0.3	>20	0.90 ± 0.04	246.6	0.74 ± 0.07
3f	3-(Trifluoromethyl)propyl	0.53 ± 0.06	>20	0.4 ± 0.1	177.0	Stable
4a		0.27 ± 0.3	>20	1.1 ± 0.1	25.7	0.43 ± 0.04

Therapeutic index is defined as the inhibitor EC$_{50}$ value against the most sensitive mammalian cell line divided by EC$_{50}$ versus *T.b. brucei*. Hemolytic potential was determined at inhibitor concentrations of 10 µM. Plasma and liver microsome assays were carried out at 37 °C.

Table 2
Inhibitor solubility and permeability

Inhibitor	PAMPA flux			Aqueous soln (µM)	Formulation soln (µM)	Formulation
	pH 3	pH 5	pH 7.4			
3b	960 ± 60	1512	1900 ± 300	16.1 ± 0.6	10,340 ± 80	5/50/0/45, pH 4.0
3c	1500 ± 100	960 ± 60	1300 ± 300	10.4 ± 0.3		10/10/40/45, pH 7.4
3d	1800 ± 800		1770 ± 60	4.2 ± 0.6		5/50/0/45, pH 7.4
3e				0.7 ± 0.1		10/10/40/45, pH 7.4
3f				0.3 ± 0.1	4060 ± 30	20/40/10/30, pH 7.4
4a				1.0 ± 0.2	890 ± 10	10/10/40/40, pH 6.0

Aqueous solubility for each compound was determined in deionized water. Formulations are shown as the ratio of ethanol/propylene glycol/PEG 400.

dosing, although micromolar levels of the O-demethylation product **3c** were transiently observed for 1–2 h following drug treatment. This is significant in that metabolite **3c** reaches trypanocidal concentrations (∼2 µM) in vivo. However, **3c** was completely oxidized to **5b** within 4 h after dosing, thus indicating that further optimization was required. The identities of metabolites **5a** and **5b** were determined by comparison to the MS/MS spectrum of a chemically synthesized sample of **5b** (Supplementary data).

It was expected that replacement of the N9 moiety with a saturated alkyl chain might improve oxidative stability, and **3e** was tested to explore this hypothesis. In vitro, this approach resulted in a significant improvement in plasma stability ($t_{1/2}$ = 246.6 h), although microsomal stability was comparable to previous compounds ($t_{1/2}$ = 0.74 h). It was not possible to determine PAMPA permeability for this compound do to its low solubility (Table 1 and 2). Stability was significantly improved in vivo, and trypanocidal concentrations (1–2 µM) of the parent compound were observed in the plasma for 1–2 h after dosing. However, by 4 h post dosing the parent inhibitor was undetectable. Three unidentified metabolites (**5c–e**) with m/z values of 511.1, 335.0, and 391.1 were observed for **3e**, and obvious oxidation products of the Ω and Ω-1 positions were not observed. These metabolites appear to be significantly less hydrophobic, as indicated by their shortened retention times by reverse-phase HPLC.

Although the site of transformation of **3e** remained unclear, oxidation and subsequent modification of either the Ω or Ω-1 carbons were thought to be the most likely scenarios. To block possible oxidation at these positions, the terminal methyl group of the **3e** *n*-butyl substituent was replaced with a trifluoromethyl group (compound **3f**). We hypothesized that eliminating available hydrogen atoms at the terminal methyl group would prevent oxidation of the Ω position, while introduction of the electronegative trifluoro-

methyl moiety would reduce p450-mediated oxidation at the Ω-1 position. This strategy was highly successful in vitro, and **3f** displayed excellent stability in both plasma ($t_{1/2}$ = 177.0 h) and microsomes (no observable transformation). In vivo performance was similarly improved, and **3f** achieved a peak plasma concentration of approximately 10 µM with no detectable metabolites at any collection time. At oral dosages tested (50, 100, 200, 400, and 1000 mg/kg), plasma concentrations of the inhibitor peaked at between 6 and 10 µM within 1–4 h of dosing (data not shown). Although peak concentration was similar for all treatment groups, time required to clear the drug increased with dosage. Following treatment with 50 or 100 mg/kg, the inhibitor was cleared within 24 h, while at dosages of 400 mg/kg or higher, inhibitor remained at micromolar concentrations for 48 h or longer. This profile suggests that the inhibitor is orally available at all tested dosages, that the peak plasma concentration of the drug is limited by its solubility, and that a high volume of distribution is likely providing a reservoir for retention of the drug in vivo. This is further supported by the peak plasma concentrations measured following IV administration of **3f** (Supplementary data) as well as the inhibitor concentrations measured in brain tissue (see below). These data suggest that the hydrophobic inhibitor partitions into other tissues after entering the circulation, and equilibrates back into the bloodstream as the drug is cleared.

To further assess the potential of **3f** as a lead compound, long-term solid state stability was tested at simulated tropical conditions (37 °C, 100% humidity) and was found to be completely stable for at least 30 days. This stability profile is promising and especially important in HAT endemic areas that often lack electricity required for climate controlled drug storage. The stability, oral availability, and plasma exposure of **3f** indicates it is a promising lead compound for HAT.

4.2. Efficacy studies

Due to the encephalopathic nature of HAT, a major concern for new drug development is CNS availability. Of the four current clinical drugs, only melarsoprol is effective against CNS stage *T.b. rhodesiense* and *T.b. gambiense* infections, and the paucity of CNS permeable drugs drives the need for drugs effective against late stage HAT. To begin assessing the potential of **3f** against parasites in the CNS, 6 mice were treated at 200 mg/kg, and plasma and brain tissue were collected to determine plasma and CNS inhibitor concentrations. Brain concentrations of **3f** paralleled those in the plasma, with concentrations peaking within 4 h, and remaining relatively constant for at least 24 h before declining by 48 h. Peak concentrations in the brain (~20 μM) were approximately 2 fold higher than those in the plasma over the first 24 h. These data indicate that the inhibitor freely crosses the BBB, and is therefore a promising lead for developing drugs against late stage HAT.

A single oral dose of 200 mg/kg established a steady peak plasma concentration for approximately 24 h, and this dosage was determined to be most suitable for a daily treatment regimen. Chronic toxicity of the inhibitor was assessed in a repeat dose study (200 mg/kg daily for 10 days) to determine an appropriate course of treatment. No toxicity was observed at any point by any of the measures used (CBC analysis, serum chemistry, functional observation battery). The toxicity of **3f** was also tested at IV dosages of 2, 4, and 8 mg/kg. Some negative symptoms were observed immediately after dosing (decreased movement and transient darkening of the eyes), but all mice recovered within 30 s and no subsequent adverse effects were observed. Following oral dosing, plasma concentrations of **3f** were approximately 20-fold higher than its EC_{50} (0.53 ± 0.06 μM) and 10-fold higher than its EC_{90} (0.8 μM) against cultured parasites. No toxicity was observed in the oral MTD study at up to 1000 mg/kg, and **3f** was determined to be a highly promising candidate for efficacy testing.

4.3. Efficacy results

Compound **3f** was evaluated for efficacy in standard murine models for acute *T.b. brucei* and *T.b. rhodesiense* infection.[13,27] In the *T.b. brucei* infection model, all mice from the control group showed significant disease progression by day 6 pi and were euthanized according to the protocol. In mice treated with **3f** (200 mg/kg) for a 5-day period beginning on day 0, 4/8 animals showed detectable parasitemia on day 4, and by day 6 only half of the mice from this group required euthanasia (Fig. 3). Two of the **3f** treated mice lived longer than 14 days, and there was a significant increase in average survival time ($p = 0.068$) for inhibitor treated animals (9.6 days) relative to the vehicle only controls (5.6 days). Parasitemia at day 4 was predictive of survival time.
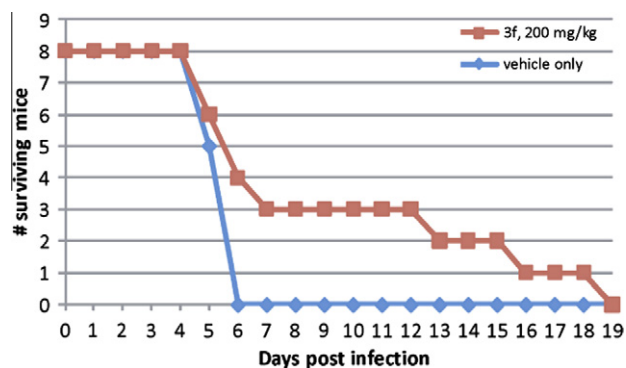

Figure 3. Mouse survival time post-infection.

All animals with measurable parasitemia at day 4 died by day 6, while the mice without detectable parasitemia lived for 7–19 days.

In the *T.b. rhodesiense* infection model mice were treated with 50, 100, or 200 mg/kg of **3f** daily on days 3–6 pi. There was no significant difference between the survival time of mice treated with vehicle only (11.5 ± 0.6 days) and those treated with **3f** (data not shown). As this result was at odds with the *T.b. brucei* findings, sensitivity of the *T.b. rhodesiense* strain used in this experiment was tested and it was found that the EC_{50} for this strain was roughly 10-fold weaker than seen with *T.b. brucei*. Thus, the pharmacodynamic result makes sense in the context of the in vitro and in vivo data.

5. Discussion

5.1. ADME studies

We observed a good correlation between inhibitor stability in mouse liver microsome preparations and actual CL in mice. The poor in vivo stability of inhibitors **3b–e** was predicted by their short half lives in this assay (between 0.4 and 1.1 h). Additionally, the microsome studies successfully predicted the **5a** metabolite for compound **3b**, but not the downstream metabolite **5b**. This discrepancy may be explained by the lack of a functional β-oxidation pathway in microsomal fractions, which is a likely route for the conversion of **5a** to **5b**. The two metabolites observed in vivo for **3c** (**5b** and the unidentified metabolite with $m/z = 386$) were identical to those observed in the microsomal assay. O-Demethylation was observed for **3d** both in vivo and in vitro, and the three metabolites of **3e** observed in this assay were identical to the three observed in mice. Only **3f** was completely stable, consistent with in vivo data. Although mouse metabolism data was not obtained for **4a** due to poor oral absorption, in liver microsomes the N9 side chain of this compound was primarily converted to the corresponding carboxylic acid ($m/z = 429$).

Due to low aqueous solubility, PAMPA data was only obtained for inhibitors **3b–d** (Table 2). Although the rapidly metabolized parent species were not observed in vivo, the metabolites of these compounds were detected at relatively high concentrations (>50 μM), suggesting good oral absorption of these inhibitors. These results are consistent with the PAMPA assay data. Therefore, for this compound series, it is fruitful to utilize the combination of in vitro microsome assays together with solubility and passive permeability models to predict the bioavailability of individual compounds.

5.2. Efficacy studies

As described above, a pharmacokinetics driven approach was used to select a candidate TbcatB inhibitor that best matched the product profile of oral availability, metabolic stability, potency, and CNS accumulation. The best candidate **3f** was then examined in murine disease models and showed activity against the cattle disease but not the human disease.

Inhibitor **3f** is somewhat less effective at delaying disease progression in a murine *T.b. brucei* infection compared to previously reported irreversible diazomethyl ketone inhibitors.[13] However, it should be noted that diazomethyl ketones require repeated IP administration at higher dosages (250 mg/kg), and that acute toxicity was a limiting factor at these dosages. The reversible purine-nitrile scaffold displays more desirable inhibition kinetics, and **3f** represents a significant improvement in terms of oral absorption and toxicity compared to the peptidyl diazomethyl ketones.

Although **3f** treatment was not curative, the clear efficacy against *T.b. brucei* in delaying disease progression coupled with the

pharmacokinetic behavior of this inhibitor demonstrates that this is a promising lead. The compound is quite stable in vivo with no detectable metabolites. Peak plasma concentration (6.5–9.7 µM) was reached within 1–4 h after oral administration for all tested dosages, and peak plasma concentration was maintained for over 24 h following a single oral dose of 200 mg/kg or more.

Infections were not cleared by treatment with **3f** in the *T.b. brucei* model, though plasma levels of the drug were maintained for nearly one week at concentrations 10-fold higher than the inhibitor's in vitro EC_{90}. It is possible that this discrepancy is due to nutrients or growth factors only present in vivo that change parasite sensitivity to inhibitor. Or, it may be the case that there is an in vivo selection for drug resistant parasites. Alternatively, it may be that the available concentration of drug in vivo is lower than expected, possibly due to differences in non-specific protein/inhibitor binding. Given the established efficacy of this inhibitor, it is likely that improving peak plasma concentration will significantly improve in vivo activity. Based on solubility and preliminary pharmacokinetic data, it is likely that the peak plasma concentration of **3f** is limited by aqueous solubility and not by in vivo stability or oral absorption. It is notable that the structurally similar carboxylic acid metabolites **5a** and **5b**, derived from inhibitors **3b–c**, achieved plasma concentrations of 50–100 µM. This suggests that it should be possible to improve **3f** plasma exposure by optimizing solubility.

3f is inactive in vivo against *T.b. rhodesiense*, presumably due to decreased potency against *T.b. rhodesiense* (EC_{50} = 4.9 µM) relative to *T.b. brucei* (EC_{50} = 0.53 µM). It is also possible that pharmacokinetic differences between the two mouse models used may have also contributed to differences in in vivo efficacy. The lack of efficacy against *T.b. rhodesiense* does not necessarily diminish the potential of the purine-nitrile scaffold against HAT, but underscores the importance of testing inhibitor potency against the human pathogen early in a development program in addition to the more commonly utilized *T.b. brucei* model.

6. Conclusion

We describe herein the optimization of a series of purine-nitrile inhibitors in order to enhance in vivo ADME parameters and to study the efficacy of these compounds in two murine models of African trypanosomiasis. Several inhibitors were tested for acute toxicity in mice, and all were determined to be non-toxic at doses up to 200 mg/kg. **3f** was found to be non-toxic at oral doses up to 1000 mg/kg. Based upon PK modeling of the initial inhibitor series, structural modifications were made to optimize for in vivo stability, and the orally available and CNS permeable inhibitor **3f** was discovered. This compound displayed peak concentrations in plasma and brain tissue of approximately 10 µM and of approximately 20 µM in brain tissue. These inhibitor levels were maintained for over 24 h following a single oral dose of 200 mg/kg. In addition, no negative symptoms were observed for this inhibitor in a chronic toxicity study in which mice were given 200 mg/kg of inhibitor daily by oral gavage for 10 consecutive days. Finally, this inhibitor was efficacious in a murine disease model, significantly extending the survival time of *T.b. brucei* infected mice relative to a vehicle control. However, the same compound was not efficacious in *T.b. rhodesiense* infected mice, most likely due to lower potency against the human parasite relative to *T.b. brucei*. This inhibitor is significant in that it represents one of the only examples of a novel anti-trypanocidal chemotype that is CNS permeable, orally available, and efficacious in vivo against *T.b. brucei*.

Supplementary data

Supplementary data associated with this article can be found, in the online version, at doi:10.1016/j.bmc.2010.09.073.

References and notes

1. WHO Human African Trypanosomiasis Drugs. http://www.who.int/trypanosomiasis_african/drugs/en/.
2. Kennedy, P. G. *J. Clin. Invest.* **2004**, *113*, 496.
3. Janssens, P. G.; De Muynck, A. *Ann. Soc. Belg. Med. Trop.* **1977**, *57*, 475.
4. Ogada, T.; Fink, E.; Mbwabi, D. *Trans. R. Soc. Trop. Med. Hyg.* **1973**, *67*, 280.
5. Mdachi, R. E.; Thuita, J. K.; Kagira, J. M.; Ngotho, J. M.; Murilla, G. A.; Ndung'u, J. M.; Tidwell, R. R.; Hall, J. E.; Brun, R. *Antimicrob. Agents Chemother.* **2009**, *53*, 953.
6. Thuita, J. K.; Karanja, S. M.; Wenzler, T.; Mdachi, R. E.; Ngotho, J. M.; Kagira, J. M.; Tidwell, R.; Brun, R. *Acta Trop.* **2008**, *108*, 6.
7. Jennings, F. W.; Urquhart, G. M. *Z. Parasitenkd* **1983**, *69*, 577.
8. Arrick, B. A.; Griffith, O. W.; Cerami, A. *J. Exp. Med.* **1981**, *153*, 720.
9. Minagawa, N.; Yabu, Y.; Kita, K.; Nagai, K.; Ohta, N.; Meguro, K.; Sakajo, S.; Yoshimoto, A. *Mol. Biochem. Parasitol.* **1997**, *84*, 271.
10. Yabu, Y.; Yoshida, A.; Suzuki, T.; Nihei, C.; Kawai, K.; Minagawa, N.; Hosokawa, T.; Nagai, K.; Kita, K.; Ohta, N. *Parasitol. Int.* **2003**, *52*, 155.
11. Chowdhury, S. F.; Villamor, V. B.; Guerrero, R. H.; Leal, I.; Brun, R.; Croft, S. L.; Goodman, J. M.; Maes, L.; Ruiz-Perez, L. M.; Pacanowska, D. G.; Gilbert, I. H. *J. Med. Chem.* **1999**, *42*, 4300.
12. Hofer, A.; Steverding, D.; Chabes, A.; Brun, R.; Thelander, L. *Proc. Natl. Acad. Sci. U.S.A.* **2001**, *98*, 6412.
13. Scory, S.; Caffrey, C. R.; Stierhof, Y. D.; Ruppel, A.; Steverding, D. *Exp. Parasitol.* **1999**, *91*, 327.
14. Troeberg, L.; Morty, R. E.; Pike, R. N.; Lonsdale-Eccles, J. D.; Palmer, J. T.; McKerrow, J. H.; Coetzer, T. H. *Exp. Parasitol.* **1999**, *91*, 349.
15. Manganaro, M.; Mascellino, M. T.; Gradoni, L. *Parasite* **2003**, *10*, 147.
16. Bitonti, A. J.; Byers, T. L.; Bush, T. L.; Casara, P. J.; Bacchi, C. J.; Clarkson, A. B., Jr.; McCann, P. P.; Sjoerdsma, A. *Antimicrob. Agents Chemother.* **1990**, *34*, 1485.
17. Mallari, J. P. S. A.; Caffrey, C.; Kosinski, A.; Connely, M.; McKerrow, J. H.; Guy, R. K. *J. Med. Chem.* **2009**, *52*, 6489.
18. Mallari, J. P.; Shelat, A. A.; Obrien, T.; Caffrey, C. R.; Kosinski, A.; Connelly, M.; Harbut, M.; Greenbaum, D.; McKerrow, J. H.; Guy, R. K. *J. Med. Chem.* **2008**, *51*, 545.
19. Mackey, Z. B.; O'Brien, T. C.; Greenbaum, D. C.; Blank, R. B.; McKerrow, J. H. *J. Biol. Chem.* **2004**, *279*, 48426.
20. O'Brien, T. C.; Mackey, Z. B.; Fetter, R. D.; Choe, Y.; O'Donoghue, A. J.; Zhou, M.; Craik, C. S.; Caffrey, C. R.; McKerrow, J. H. *J. Biol. Chem.* **2008**, *283*, 28934.
21. Di, L.; Kerns, E. H.; Li, S. Q.; Petusky, S. L. *Int. J. Pharm.* **2006**, *317*, 54.
22. Ionsource Principles of MS Quantitation. http://www.ionsource.com/tutorial/msquan/requantoc.htm.
23. Institute of Laboratory Animals, G. S. o. M., Kyoto-University, Japan Kyoto Rat Phenotype Database, The National Bioresource Project for the Rat in Japan. http://www.anim.med.kyoto-u.ac.jp/NBR/strainsx/FOB_menue.aspx.
24. Shin, S. Y.; Lee, S. H.; Yang, S. T.; Park, E. J.; Lee, D. G.; Lee, M. K.; Eom, S. H.; Song, W. K.; Kim, Y.; Hahm, K. S.; Kim, J. I. *J. Pept. Res.* **2001**, *58*, 504.
25. Blanchard, J. *J. Chromatogr.* **1981**, *226*, 455.
26. Clarke, S. E.; Jeffrey, P. *Xenobiotica* **2001**, *31*, 591.
27. Abdulla, M. H.; O'Brien, T.; Mackey, Z. B.; Sajid, M.; Grab, D. J.; McKerrow, J. H. *PLoS Negl. Trop. Dis.* **2008**, *2*, e298.